Inorg. Chem. **2007**, *46*, 740–749

DNA Binding and Cytotoxicity of Ruthenium(II) and Rhenium(I) Complexes of 2-Amino-4-phenylamino-6-(2-pyridyl)-1,3,5-triazine

Dik-Lung Ma,[†,‡] Chi-Ming Che,*[,†] Fung-Ming Siu,[†] Mengsu Yang,[§] and Kwok-Yin Wong[‡]

Department of Chemistry and Open Laboratory of Chemical Biology of the Institute of Molecular Technology for Drug Discovery and Synthesis, The University of Hong Kong, Pokfulam Road, Hong Kong SAR, China, Department of Biology and Chemistry, City University of Hong Kong, 83 Tat Chee Avenue, Kowloon, Hong Kong SAR, China, and Department of Applied Biology and Chemical Technology and Central Laboratory of the Institute of Molecular Technology for Drug Discovery and Synthesis, The Hong Kong Polytechnic University, Hunghom, Kowloon, Hong Kong, China

Received August 11, 2006

[Ru(^{t}Bu$_2$bpy)$_2$(2-appt)](PF$_6$)$_2$ [**1**·(PF$_6$)$_2$, ^{t}Bu$_2$bpy = 4,4′-di-*tert*-butyl-2,2′-bipyridine, 2-appt = 2-amino-4-phenylamino-6-(2-pyridyl)-1,3,5-triazine] and [Re(CO)$_3$(2-appt)Cl] (**2**) were prepared and characterized by X-ray crystal analysis. The binding of **1**·(PF$_6$)$_2$ and **2** to calf thymus DNA (ct DNA) led to increases in the DNA melting temperature (ΔT_m = +12 °C), modest hypochromism (29% and 5% of the absorption bands at λ_{max} = 450 and 376 nm, respectively), and insignificant shifts in the absorption maxima. The binding constants of **1**·(PF$_6$)$_2$ and **2** with ct DNA, as determined by absorption titration, are (8.9 ± 0.5) × 10^4 and (3.6 ± 0.1) × 10^4 dm^3 mol^{-1}, respectively. UV–vis absorption titration, DNA melting studies, and competition dialysis using synthetic oligonucleotides [poly(dA–dT)$_2$ and poly(dG–dC)$_2$] revealed that **1**·(PF$_6$)$_2$ and **2** exhibit a binding preference for AT sequences. A modeling study on the interaction between **1** or **2** and B-DNA revealed that the minor groove is the most favored binding site and an extensive hydrogen-bonding network is formed. As determined by MTT assays, **1**·(PF$_6$)$_2$ and **2** exhibited moderate cytotoxicities toward several human cancer cell lines (KB-3-1, HepG2, and HeLa), as well as a multi-drug-resistant cancer cell line (KB-V-1). According to confocal microscopic and flow cytometric studies, **1**·(PF$_6$)$_2$ and **2** induced apoptosis (50–60%) in cancer cells with <5% necrosis detected.

Introduction

In the development of novel metal-based therapeutics, detailed studies on the interactions between biomolecular targets such as DNA and structurally defined transition-metal complexes can provide invaluable information.[1] It has been well documented that metal complexes can bind to DNA covalently as well as noncovalently.[2,3] Organometallic ruthenium(II)−arene complexes [(η^6-arene)Ru(XY)Cl]$^+$ [arene = biphenyl, XY = ethylenediamine (en)] are recent reported examples of the former, in that they bind to DNA covalently, presumably through the coordination of the Ru atom to the N7 position of guanine bases.[1e−j] Furthermore, these ruthenium(II)−arene complexes have also been reported to exhibit anticancer activity in both in vitro and in vivo studies.[1e−h] Noncovalent interactions between transition-metal complexes and DNA can occur by intercalation, groove binding, or external electrostatic binding. Lippard and co-workers pioneered work in this area through the study of the intercalation of square-planar d^8 Pt^{II} complexes with DNA.[1a] In addition, Barton and co-workers reported that a number of octahedral

* To whom correspondence should be addressed. Fax: +(852)2857-1586. E-mail: cmche@hku.hk.
† The University of Hong Kong.
‡ The Hong Kong Polytechnic University
§ City University of Hong Kong.

(1) (a) Howe-Grant, M.; Lippard, S. J. *Biochemistry* **1979**, *18*, 5762. (b) Jamieson, E. R.; Lippard, S. J. *Chem. Rev.* **1999**, *99*, 2467. (c) Claussen, C. A.; Long, E. C. *Chem. Rev.* **1999**, *99*, 2797. (d) Clarke, M. J.; Zhu, F.; Frasca, D. R. *Chem. Rev.* **1999**, *99*, 2511. (e) Morris, R. E.; Aird, R. E.; Murdoch, P. D.; Chen, H. M.; Cummings, J.; Hughes, N. D.; Parsons, S.; Parkin, A.; Boyd, G.; Jodrell, D. I.; Sadler, P. J. *J. Med. Chem.* **2001**, *44*, 3616. (f) Aird, R. E.; Cummings, J.; Ritchie, A. A.; Muir, M.; Morris, R. E.; Chen, H.; Sadler, P. J.; Jodrell, D. I. *Br. J. Cancer* **2002**, *86*, 1652. (g) Yan, K. Y.; Melchart, M.; Habtemariam, A.; Sadler, P. J. *Chem. Commun.* **2005**, 4764. (h) Novakova, O.; Chen, H. M.; Vrana, O.; Rodger, A.; Sadler, P. J.; Brabec, V. *Biochemistry* **2003**, *42*, 11544. (i) Chen, H. M.; Parkinson, J. A.; Parsons, S.; Coxall, R. A.; Gould, R. O.; Sadler, P. J. *J. Am. Chem. Soc.* **2002**, *124*, 3064. (j) Chen, H. M.; Parkinson, J. A.; Morris, R. E.; Sadler, P. J. *J. Am. Chem. Soc.* **2003**, *125*, 173.

10.1021/ic061518s CCC: $37.00
Published on Web 01/12/2007

d^6-metal complexes containing aromatic diimine ligands[4] could act as photoluminescent metal-based probes for the study of DNA binding. $[Ru(diimine)_3]^{2+}$,[4,5] $[Cu(diimine)_2]^{+}$,[6] and $[Pt(terpy)L]^{+}$ [7,8] (terpy = 2,2′:6′,2″-terpyridine, L = anionic/neutral ligand) are examples of metal complexes that have been reported to bind DNA through $\pi-\pi$ and/or electrostatic interactions. However, there are few reported examples of crescent-shaped complexes that contain the appropriately orientated H-bonding functionalities to permit effective binding to either the major or minor grooves of DNA.[9]

As part of our ongoing efforts to develop novel inorganic medicines, we have been working toward the synthesis of metal complexes containing π-conjugated organic ligands, with or without H-bonding motifs, that are capable of binding to DNA in a predetermined manner. In this regard, we were attracted to Mingos and co-workers' studies on metal complexes containing nitrogen-donor ligands such as 2-appt [2-amino-4-phenylamino-6-(2-pyridyl)-1,3,5-triazine] that can participate in both hydrogen-bonding and $\pi-\pi$ interactions.[10] Herein, we describe the DNA binding reactions of $[Ru(^tBu_2bpy)_2(2\text{-appt})](PF_6)_2$ [**1**·$(PF_6)_2$] and $[Re(CO)_3(2\text{-appt})Cl]$ (**2**) (Chart 1). We also report the cytotoxicities of these two complexes toward a number of cancer cell lines.

Chart 1. Schematic Drawings of $[Ru(^tBu_2bpy)_2(2\text{-appt})]^{2+}$ (**1**) and $[Re(CO)_3(2\text{-appt})Cl]$ (**2**)

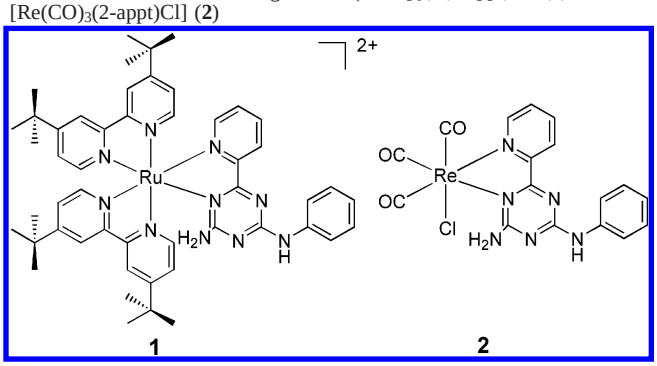

Experimental Section

Materials. Calf thymus DNA (ct DNA) was purchased from Sigma Chemical Co. Ltd. and purified as described elsewhere.[11] Poly(dG−dC)$_2$ and poly(dA−dT)$_2$ (Sigma Chemical Co. Ltd.) were used as received. Two complementary oligonucleotides, 5′-GCTCCCCTTTCTTGCGGAGATTCTCTTCCTCTG-3′ and 5′-CAGAGGAAGAGAATCTCCGCAAGAAAGGGGAGC-3′, were obtained from DNAgency (Malvern, PA) and annealed to give a double-stranded 33-bp DNA. The purity of the 33-bp DNA was checked by electrophoresis on a 20% polyacrylamide gel. The DNA concentration per base pair was determined by UV−vis absorption spectroscopy. The following molar extinction coefficients (bp cm^{-1} M^{-1}) at the indicated wavelengths were used: calf thymus DNA, $\epsilon_{260} = 13\,200$; poly(dG−dC)$_2$, $\epsilon_{254} = 16\,800$; poly(dA−dT)$_2$, $\epsilon_{260} = 12\,000$.[12] A plasmid DNA, pDR2 (10.7 kb), was purchased from Clontech Laboratories Inc. (Palo Alto, CA). Unless otherwise stated, DNA binding studies were performed in degassed Tris buffer (5 mM Tris, 50 mM NaCl, pH 7.2) at 20 °C. 2-Amino-4-phenylamino-6-(2-pyridyl)-1,3,5-triazine (2-appt)[13] and *cis*-$[Ru(^tBu_2bpy)_2Cl_2]$[14] ($^tBu_2bpy$ = 4,4′-di-*tert*-butyl-2,2′-bipyridine) were prepared as described previously.

The parental epidermal carcinoma KB-3-1 cell line and the multidrug-resistant KB-V-1 cell line (derived from KB-3-1 cells by a series of stepwise selections against the anticancer agent vinblastin) were provided by Dr. Michael Gottesman of National Institute of Health, Bethesda, MD,[15,16] and maintained in the presence of 1 μg/

(2) (a) Liu, H. Q.; Peng, S. M.; Che, C. M. *J. Chem. Soc., Chem. Commun.* **1995**, 509. (b) Liu, H. Q.; Cheung, T. C.; Peng, S. M.; Che, C. M. *J. Chem. Soc., Chem. Commun*. **1995**, 1787. (c) Liu. H. Q.; Cheung, T. C.; Che, C. M. *Chem. Commun*. **1996**, 1039. (d) Wu, L. Z.; Cheung, T. C.; Che, C. M.; Cheung, K. K.; Lam, M. H. W. W. *Chem. Commun.* **1998**, 1127. (e) Che, C. M.; Yang, M.; Wong, K. H.; Chan, H. L.; Lam, W. *Chem. Eur. J.* **1999**, *5*, 3350. (f) Chan, H. L.; Ma, D. L.; Yang, M.; Che, C. M. *ChemBioChem* **2003**, *4*, 62. (g) Ma, D. L.; Che, C. M. *Chem. Eur. J.* **2003**, *9*, 6133. (h) Che, C. M.; Sun, R. W.-Y.; Yu, W. Y.; Ko, C.-B.; Zhu, N. Y.; Sun, H. Z. *Chem. Commun.* **2003**, 1718.

(3) (a) Sundquist, W. I.; Lippard, S. J. *Coord. Chem. Rev.* **1990**, *100*, 293. (b) Cusumano, M.; Di Pietro, M. L.; Giannetto, A.; Nicolò, F.; Rotondo, E. *Inorg. Chem.* **1998**, *37*, 563. (c) Sigman, D. S.; Mazumder, A.; Perrin, D. M. *Chem. Rev.* **1993**, *93*, 2295. (d) Stoeffler, H. D.; Thornton, N. B.; Temkin, S. L.; Schanze, K. S. *J. Am. Chem. Soc.* **1995**, *117*, 7119. (e) Holmlin, R. E.; Dandliker, P. J.; Barton, J. K. *Angew. Chem., Int. Ed.* **1997**, *36*, 2715. (f) Metcalfe, C.; Thomas, J. A. *Chem. Soc. Rev.* **2003**, *32*, 215.

(4) (a) Kumar, C. V.; Barton, J. K.; Turro, N. J. *J. Am. Chem. Soc.* **1985**, *107*, 5518. (b) Friedman, A. E.; Chambron, J. C.; Sauvage, J. P.; Turro, N. J.; Barton, J. K. *J. Am. Chem. Soc.* **1990**, *112*, 4960. (c) Dupureur, C. M.; Barton, J. K. *J. Am. Chem. Soc.* **1994**, *116*, 10286. (d) Dupureur, C. M.; Barton, J. K. *Inorg. Chem.* **1997**, *36*, 33. (e) Holmlin, R. E.; Stemp, E. D. A.; Barton, J. K. *Inorg. Chem.* **1998**, *37*, 29. (f) Erkkila, K. E.; Odom, D. T.; Barton, J. K. *Chem. Rev.* **1999**, *99*, 2777.

(5) (a) Greguric, I.; Aldrich-Wright, J. R.; Collins, J. G. *J. Am. Chem. Soc.* **1997**, *119*, 3621. (b) Tuite, E.; Lincoln, P.; Norden, B. *J. Am. Chem. Soc.* **1997**, *119*, 239. (c) Moucheron, C.; Kirsch-De, Mesmaeker, A.; Kelly, J. M. *J. Photochem. Photobiol. B* **1997**, *40*, 91. (d) Lincoln, P.; Norden, B. *J. Phys. Chem. B* **1998**, *102*, 9583. (e) Proudfoot, E. M.; Mackay, J. P.; Karuso, P. *Biochemistry* **2001**, *40*, 4867.

(6) (a) Sigman, D. S. *Acc. Chem. Res*. **1986**, *19*, 180. (b) McMillin, D. R.; McNett, K. M. *Chem. Rev.* **1998**, *98*, 1201.

(7) (a) Jennette, K. W.; Lippard, S. J.; Vassilia, G. A.; Bauer, W. R. *Proc. Natl. Acad. Sci. U.S.A.* **1974**, *71*, 3839. (b) Howe-Grant, M.; Wu, K. C.; Bauer, W. R.; Lippard, S. J. *Biochemistry* **1976**, *15*, 4339. (c) Wang, A. H. J.; Nathans, J.; van der Marel, G.; van Boom, J. H.; Rich, A. *Nature* **1978**, *276*, 471. (d) Norden, B. *Inorg. Chim. Acta* **1978**, *31*, 83. (e) Barton, J. K.; Lippard, S. J. *Biochemistry* **1979**, *18*, 2661. (f) Wakelin, L. P. G.; McFadyen, W. D.; Walpole, A. G.; Roos, I. A. *Biochem. J.* **1984**, *222*, 203. (g) Arena, G.; Scolaro, L. M.; Pasternack, R. F.; Romeo, R. *Inorg. Chem.* **1995**, *34*, 2994. (h) Peyratout, C. S.; Aldridge, T. K.; Crites, D. K.; McMillin, D. R. *Inorg. Chem*. **1995**, *34*, 4484. (i) McCoubrey, A.; Latham, H. C.; Cook, P. R.; Rodger, A.; Lowe, G. *FEBS Lett.* **1996**, *380*, 73. (j) Cusumano, M.; Di, Pietro, M. L.; Giannetto, A.; Romano, F. *Inorg. Chem.* **2000**, *39*, 50.

(8) (a) Lippard, S. J. *Acc. Chem. Res.* **1978**, *11*, 211. (b) McFadyen, W. D.; Wakelin, L. P. G.; Roos, I. A. G.; Leopold, V. A. *J. Med. Chem.* **1985**, *28*, 1113. (c) Lowe, G.; Droz, A. S.; Vilaivan, T.; Weaver, G. W.; Park, J. J.; Pratt, J. M.; Tweedale, L.; Kelland, L. R. *J. Med. Chem.* **1999**, *42*, 3167. (d) Lowe, G.; Droz, A. S.; Vilaivan, T.; Weaver, G. W.; Tweedale, L.; Pratt, J. M.; Rock, P.; Yardley, V.; Croft, S. L. *J. Med. Chem.* **1999**, *42*, 999. (e) Todd, J. A.; Rendina, L. M. *Inorg. Chem.* **2002**, *41*, 3331.

(9) (a) Dervan, P. B.; Burli, R. W. *Curr. Opin. Chem. Biol.* **1999**, *3*, 688. (b) Liu, J.-G.; Ye, B.-H.; Li, H.; Zhen, Q.-X.; Ji, L.-N.; Fu, Y.-H. *J. Inorg. Biochem.* **1999**, *76*, 265. (c) Maheswari, P. U.; Palaniandavar, M. *J. Inorg. Biochem.* **2004**, *98*, 219. (d) Caspar, R.; Musatkina, L.; Tatosyan, A.; Amouri, H.; Gruselle, M.; Guyard-Duhayon, C.; Duval, R.; Cordier, C. *Inorg. Chem.* **2004**, *43*, 7986.

(10) Burrows, A. D.; Chan, C. W.; Chowdhry, M. M.; McGrady, J. E.; Mingos, D. M. P. *Chem. Soc. Rev.* **1995**, *24*, 329.

(11) Sambrook, J.; Fritsch, E. F.; Maniatis, T. *Molecular Cloning: A Laboratory Manual*, 2nd ed.; Cold Spring Harbor Laboratory Press: Woodbury, NY, 1989; pp E.3 and E.10.

(12) Felsenfeld, G.; Hirschman, S. Z. *J. Mol. Biol.* **1965**, *13*, 407.

(13) Chan, C.-W.; Mingos, D. M. P.; White, A. J. P.; Williams, D. J. *Polyhedron* **1996**, *15*, 1753.

(14) BenHadda, T.; Le Bozec, H. *Polyhedron* **1988**, *7*, 575.

(15) Akiyama, S. I.; Fojo, A.; Hanover, J. A.; Pastan, I.; Gottesman, M. M. *Somat. Cell Mol. Genet.* **1985**, *11*, 117.

mL vinblastin. The HepG2 (hepatocellular cancer)[17] cell line was provided by Prof. W. F. Fong of City University of Hong Kong, Hong Kong SAR. CCD-19Lu (normal lung fibroblast) and HeLa (human cervix epitheloid carcinoma) cells were obtained from American Type Culture Collection. The cell proliferation Kit I (MTT) from Roche was used to evaluate cytotoxicities.

[Ru(^{t}Bu$_2$bpy)$_2$(2-appt)](PF$_6$)$_2$ [1·(PF$_6$)$_2$]. A mixture of *cis*-[Ru(^{t}Bu$_2$bpy)$_2$Cl$_2$] (0.05 g, 0.10 mmol) and $AgCF_3SO_3$ (1.72 g, 0.19 mmol) in acetone (10 mL) was stirred at 25 °C for 3 h. The dark red mixture was filtered to remove the insoluble AgCl. The filtrate was rotary evaporated to dryness to give *cis*-[Ru(^{t}Bu$_2$bpy)$_2$(acetone)$_2$](OTf)$_2$ (45 mg), which was treated with 2-appt (0.03 g, 0.12 mmol) in refluxing methanol (10 mL) for 24 h. After the mixture had cooled to room temperature, methanolic NH_4PF_6 solution (0.10 g, 0.65 mmol in 1 mL) was added to give a red solid complex, which was recrystallized by diffusing diethyl ether into an acetonitrile solution. Yield: 0.047 g, 70%. FAB-MS: *m*/*z* 1047 $[M + PF_6]^+$. ^{1}H NMR (300 MHz, CD_3CN): 1.34 (s, 9H), 1.39 (s, 9H), 1.42 (m, 18H), 6.55 (s, 2H), 6.79 (m, 3H), 7.05 (m, 1H), 7.17 (m, 2H), 7.36 (m, 2H), 7.46 (m, 6H), 7.75 (m, 1H), 8.07 (m, 1H), 8.38 (m, 1H), 8.49 (m, 4H), 8.66 (m, 1H). IR (Nujol mull/cm^{-1}): 3383 (w, ν_{N-H}), 1597 (s, $\nu_{C=N}$). Anal. Calcd for $C_{50}H_{60}N_{10}P_2F_{12}Ru$: C, 50.4; H, 5.08; N, 11.8. Found: C, 50.2; H, 5.07; N, 11.5. UV−vis (CH_3CN): λ/nm (ϵ_{max}/dm^3 mol^{-1} cm^{-1}) 450 (1.24×10^4), 283 (7.21×10^4), 215 (5.77×10^4).

[Re(CO)$_3$(2-appt)Cl] (2). A suspension of $[Re(CO)_5Cl]$ (0.08 g, 0.22 mmol) and 2-appt (0.06 g, 0.22 mmol) in methanol (20 mL) was refluxed for 24 h. After the reaction mixture had cooled to room temperature, it was concentrated to ca. 5 mL by rotary evaporation. Addition of diethyl ether gave a yellow solid complex, which was washed with CH_2Cl_2 and hexane and recrystallized from a MeCN−Et_2O mixture. Yield: 0.11 g, 84%. FAB-MS: *m*/*z* 570 $[M]^+$, 535 $[M - Cl]^+$. ^{1}H NMR (300 MHz, CD_3CN): 6.64 (s, 2H), 7.20 (m, 1H), 7.41 (m, 2H), 7.77 (m, 3H), 8.35 (m, 1H), 8.61 (m, 1H), 9.14 (m, 1H), 9.59 (m, 1H). IR (Nujol mull/cm^{-1}): 3310 (w, ν_{N-H}), 1946 (s, ν_{CO}), 1930 (s, ν_{CO}), 1602 (s, $\nu_{C=N}$). Anal. Calcd for $C_{17}H_{12}N_6O_3ClRe$: C, 35.8; H, 2.12; N, 14.7. Found: C, 36.1; H, 2.12; N, 14.7. UV−vis (CH_3CN): λ/nm (ϵ_{max}/dm^3 mol^{-1} cm^{-1}) 376 (5.9×10^3), 266 (3.00×10^4).

Physical Measurements. Absorption spectra were recorded on a Perkin-Elmer Lambda 19 UV−visible spectrophotometer. Emission spectra were recorded on a SPEX Fluorolog-2 model fluorescence spectrophotometer. Emission lifetime measurements were performed with a Quanta Ray DCR-3 pulsed Nd:YAG laser system (pulse output 355 nm, 8 ns). Error limits were estimated as follows: λ, ±1 nm; τ, ±10%; ϕ, ±10%). ^{1}H NMR spectra were recorded on a Bruker DPX-300 or DPX-500 NMR spectrometer. Positive-ion FAB mass spectra were recorded on a Finnigan MAT95 mass spectrometer. UV melting studies were performed using a Perkin-Elmer Lambda 900 UV−visible spectrophotometer equipped with a Peltier PTP-6 temperature programmer. Viscosity experiments were performed on a Cannon−Manning Semi-Micro viscometer immersed in a thermostated water bath maintained at 27 °C.[18a,b] Ruthenium and rhenium analyses were performed on an Agilent 7500 inductively coupled plasma mass spectrometer.

Table 1. Crystal Structure Determination Data for **1**·(PF$_6$)$_2$ and **2**

	1·(PF$_6$)$_2$·MeCN·0.5Et$_2$O	**2**
formula	$C_{54}H_{67}F_{12}N_{11}O_{0.5}P_2Ru$	$C_{17}H_{12}N_6O_3ClRe$
mol wt	1269.20	569.98
crystal system	triclinic	monoclinic
space group	$P\bar{1}$	$P2/c$ (No. 13)
a (Å)	13.356(3)	13.800(2)
b (Å)	14.821(3)	8.022(2)
c (Å)	17.251(4)	18.044(3)
α (deg)	77.47(3)	90
β (deg)	75.69(3)	102.84(2)
γ (deg)	67.17(3)	90
V (Å^3)	3021.5(12)	1947.6(6)
Z	2	4
F(000)	1308	1088
D_c (g cm^{-3})	1.395	1.944
temperature (K)	300(2)	273.2
λ (Å)	0.7107	0.7107
no. of variables	662	253
no. of unique data points	8189	3660
no. with $I > 3\sigma(I)$	6047	3170
R	0.096	0.047
wR	0.26	0.061
GOF	1.13	2.33

X-ray Structure Determination of [Ru(^{t}Bu$_2$bpy)$_2$(2-appt)](PF$_6$)$_2$ [1·(PF$_6$)$_2$] and [Re(CO)$_3$(2-appt)Cl] (2). The diffraction data were collected on a MAR diffractometer with a 300-mm image plate detector at 300 K using graphite-monochromatized Mo Kα radiation ($\lambda = 0.7107$ Å). The structures were refined by full-matrix least-squares against F_o^2 using the program SHELXL-97.[19] Crystal refinement data are listed in Table 1. Perspective views of **1**·(PF$_6$)$_2$ and **2** are presented in Figures 1 and 2, respectively. Figures S1 and S2 in the Supporting Information show crystal packing diagrams for the two complexes.

Restriction Endonuclease Fragmentation Assay. Digestion of a plasmid DNA (pDR2, 10.7 kb) with a restriction enzyme, *Apa* I (Boehringer Mannheim), was performed by mixing pDR2 (21 nM bp^{-1}) in 1× SuRE/Cut Buffer A with *Apa* I (1 unit/μL) and then incubating the mixture at 37 °C for 1 h.[20] The mixture of pDR2 with ethidium bromide (4 μM), Hoechst 33342 (200 μM), cisplatin (*cis*-Pt(NH$_3$)$_2$Cl$_2$) (200 μM), **1**·(PF$_6$)$_2$ or **2** (2−200 μM), and pDR2 (10.7 kbp, 21 nM bp^{-1}) was first incubated at room temperature for 5 min, and then restriction enzyme (1 unit/μL) was added. Solutions of pDR2 both in the absence and in the presence of the *Apa* I restriction enzyme in digestion buffer were used as controls. All solutions were incubated at 37 °C for 1 h. After restriction enzyme digestion, the samples were analyzed by agarose gel electrophoresis.

Absorption Titration. ct DNA solutions of various concentrations (0−2000 μM bp^{-1}) were added to the metal complexes [50 μM dissolved in Tris buffer (5 mM Tris, 50 mM NaCl, pH 7.2)]. Absorption spectra were recorded after equilibration at 20.0 °C for 10 min. The intrinsic binding constant, K, was determined from a plot of $D/\Delta\epsilon_{ap}$ vs D according to eq 1[21]

$$D/\Delta\epsilon_{ap} = D/\Delta\epsilon + 1/(\Delta\epsilon \times K) \quad (1)$$

(16) Shen, D. W.; Cardarelli, C.; Hwang, J.; Cornwell, M.; Richert, N.; Ishii, S.; Pastan, I.; Gottesman, M. M. *J. Biol. Chem.* **1986**, *261*, 7762.
(17) Busch, S. J.; Barnhart, R. L.; Martin, G. A.; Flanagan, M. A.; Jackson, R. L. *J. Biol. Chem*. **1990**, *265*, 22474.
(18) (a) Cohen, G.; Eisenberg, H. *Biopolymers* **1969**, *8*, 45. (b) Chaires, J. B.; Dattagupta, N.; Crothers, D. M. *Biochemistry* **1982**, *21*, 3933. (c) O'Reilly, F. M.; Kelly, J. M.; Kirsch-De Mesmaeker, A. *J. Chem. Soc., Chem. Commun.* **1996**, 1013. (d) O'Reilly, F. M.; Kelly, J. M. *J. Phys. Chem. B* **2000**, *104*, 7206.
(19) Sheldrick, G. M. *SHELXS-97, Program for Crystal Structure Analysis*; University of Göttingen: Göttingen, Germany, 1997.
(20) Sambrook, J.; Fritsch, E. F.; Maniatis, T. *Molecular Cloning: A Laboratory Manual*, 2nd ed.; Cold Spring Harbor Laboratory Press: Woodbury, NY, 1989; p 5.31.
(21) Kumar, C. V.; Asuncion, E. H. *J. Am. Chem. Soc.* **1993**, *115*, 8547.

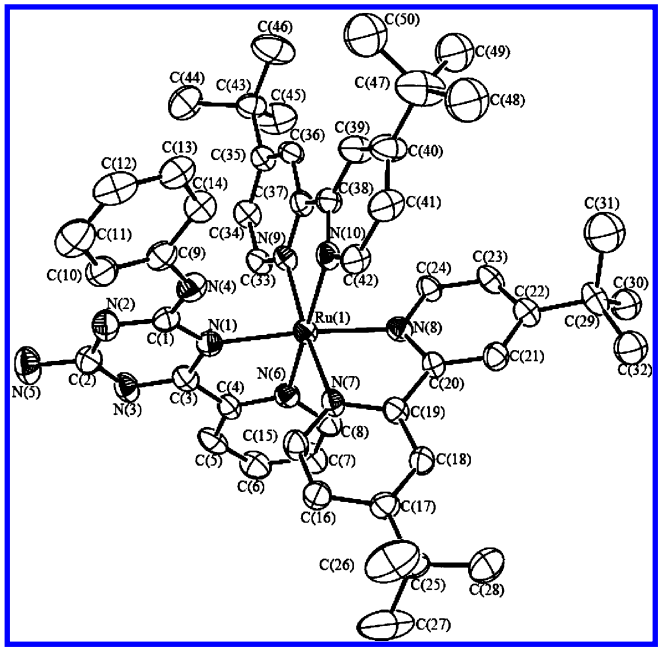

Figure 1. Perspective view of the $[Ru(^tBu_2bpy)_2(2\text{-appt})]^{2+}$ (**1**) cation (50% probability ellipsoids, hydrogen atoms omitted for clarity). Selected bond lengths (Å): Ru(1)−N(1) 2.118(6), Ru(1)−N(6) 2.060(6), Ru(1)−N(8) 2.077(7), Ru(1)−N(10) 2.107(6). Selected bond angles (deg): N(6)−Ru(1)−N(8) 98.3(2), N(6)−Ru(1)−N(10) 172.6(2), N(1)−Ru(1)−N(9) 86.5(2), N(1)−Ru(1)−N(7) 97.7(2).

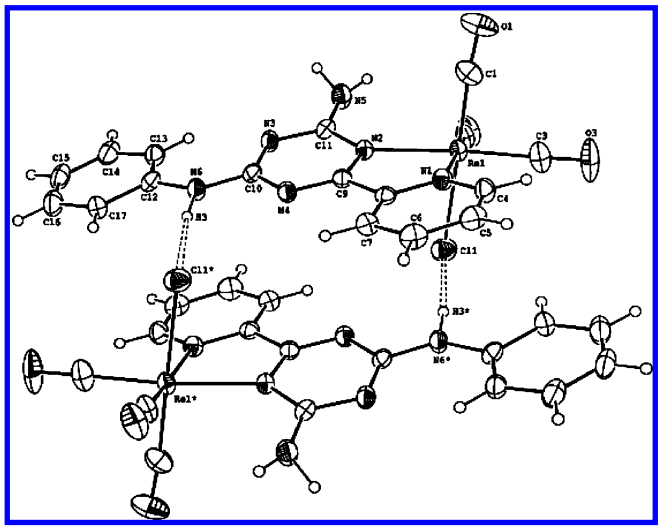

Figure 2. Perspective view of $[Re(CO)_3(2\text{-appt})Cl]$ (**2**). Selected bond lengths (Å): Re(1)−N(1) 2.167(6), Re(1)−N(2) 2.200(4), Re(1)−Cl(1) 2.497(2), Re(1)−C(1) 1.887(7). Selected bond angles (deg): Cl(1)−Re(1)−N(1) 84.0(2), Cl(1)−Re(1)−C(1) 178.8(2), N(1)−Re(1)−C(1) 97.0(2), N(1)−Re(1)−N(2) 74.7(2).

where D is the concentration of DNA in base pairs; $\Delta\epsilon_{ap} = |\epsilon_A - \epsilon_F|$; $\epsilon_A = A_{obs}/[\text{complex}]$; and $\Delta\epsilon = |\epsilon_B - \epsilon_F|$, with ϵ_B and ϵ_F corresponding to the extinction coefficients of the DNA-bound complex and unbound complex, respectively.

DNA Melting Study. Solutions of the 33-bp double-helical DNA molecule (50 μM bp^{-1}) both in the absence and in the presence of the metal complexes (DNA base pair/metal complex = 1:1) were prepared in Tris buffer. The temperature of the solution was increased at a rate of 1 °C min^{-1}, and the absorbance at 260 nm was monitored. T_m values were determined from plots of absorbance vs temperature.

Competition Dialysis Assay.[22a] Dialysate solutions (6 mM Na_2HPO_4, 2 mM NaH_2PO_4, 1 mM Na_2EDTA, and 41 mM NaCl, pH 7.0) containing 1 μM metal complex were used for the competition dialysis experiments. Each DNA sample (200 μL at 75 μM monomeric unit) was pipetted into an individual dialyzer unit (Pierce). Four dialysis units were placed in a beaker containing 400 mL of dialysate solution. The beaker was covered with Parafilm and wrapped in foil. The solution was equilibrated by continuous stirring at room temperature (20−22 °C) for 48 h. At the end of the equilibration period, DNA samples were transferred to microfuge tubes and treated with 1% SDS. The concentration of metal complex (C_t) within each dialysis unit and the free metal complex concentration (C_f) that remained in dialysate solution were each determined spectrophotometrically. The concentration of bound metal complex (C_b) was determined according to eq 2

$$C_t - C_f = C_b \tag{2}$$

Viscosity Experiments. Titrations were performed by adding **1**·$(PF_6)_2$ or **2** to ct DNA in BPE buffer (6 mM Na_2HPO_4, 2 mM NaH_2PO_4, 1 mM Na_2EDTA, and 41 mM NaCl, pH 7.0). The DNA concentration was approximately 1 mM (in base pairs). Mixing of the solution in the viscometer was achieved by briefly bubbling nitrogen gas through it. The relative viscosity of DNA in the presence and absence of the metal complex was calculated using eq 3

$$\eta = (t - t_o)/t_o \tag{3}$$

where t is the flow time of the DNA-containing solution and t_o is the flow time of buffer alone. According to Cohen and Eisenberg,[18a] the relationship between the relative solution viscosity (η/η_o) and contour length (L/L_o) is given by eq 4

$$L/L_o = (\eta/\eta_o)^{1/3} \tag{4}$$

where L_o and η_o denote the apparent molecular length and solution viscosity, respectively, in the absence of the metal complex.

Cytotoxicity Tests [MTT (3-(4,5-Dimethylthiazol-2-yl)-2,5-tetrazolium Bromide) Assays]. Cells (20 000 cells/well) were seeded in a 96-well flat-bottomed microplate containing 150 μL of growth medium [10% fetal calf serum (FCS, Gibco), 1% Sigma A-7292 Antibiotic and Antimycotic Solution in minimal essential medium (MEM-Eagle, Sigma)]. Complex **1**·$(PF_6)_2$, complex **2**, and cisplatin (positive control) were dissolved in DMSO (dimethyl sulfoxide) and mixed with the growth medium (final percentage of DMSO ≤ 4%). The microplate was incubated at 37 °C with 5% CO_2/95% air in a humidified incubator for 48 h. After incubation, 10 μL of MTT reagent (5 mg/mL) was added to each well. The microplate was re-incubated for 4 h, with 100 μL of solubilization solution (10% SDS in 0.01 M HCl) added to each well. The microplate was then left in the incubator for 24 h, before the absorbance at 550 nm was measured using a microplate reader. The IC_{50} values (concentrations required to reduce the absorbance by 50% compared to the controls) for **1**·$(PF_6)_2$ and **2** were determined by dose dependence of surviving cells after exposure to the metal complexes for 48 h.

Molecular Modeling. Molecular docking was performed using the ICM-Pro 3.4-8a program (Molsoft). To simplify the calculation, no force field of the metal atom was input in the calculations. In

(22) (a) Sun, D.; Hurley, L. H.; von Hoff, D. D. *Biotechniques* **1998**, *25*, 1046. (b) McKeage, M. J.; Berners-Price, S. J.; Galettis, P.; Bowen, R. J.; Brouwer, W.; Ding, L.; Zhuang, L.; Baguley, B. C. *Cancer Chemother. Pharmacol.* **2000**, *46*, 343.

Table 2. UV−Vis Absorption Data for **1**·$(PF_6)_2$ and **2** and Solution Emission Data for **1**·$(PF_6)_2$ in Various Solvents at 298 K

	1·$(PF_6)_2$			**2**
solvent	absorption λ/nm (ϵ_{max}/dm^3 mol^{-1} cm^{-1})	emission[a] λ_{max}/nm	ϕ_{em}[b]	absorption λ/nm (ϵ_{max}/dm^3 mol^{-1} cm^{-1})
MeCN	215 (57000), 283 (72100), 450 (12400)	646	0.001	266 (30000), 376 (br, 5900), 440 (sh, 1200)
MeOH	218 (66000), 283 (93000), 451 (16900)	640	0.0007	266 (27800), 374 (br, 5700), 440 (sh, 1200)
EtOH	215 (57000), 283 (72000), 451 (12900)	635	0.0013	268 (28900), 376 (br, 5900), 440 (sh, 1300)
CH_2Cl_2	215 (57000), 283 (73000), 450 (12500)	640	0.001	269 (30200), 383 (br, 5200), 440 (sh, 1200)

[a] Excitation at 450 nm. [b] Emission lifetime $\leq$ 0.1 μs.

other words, a soft "static" (or "frozen") approximation was kept for DNA and the metal atom during the calculation. According to the ICM method, the molecular system was described using internal coordinates as variables. The biased-probability Monte Carlo (BPMC) minimization procedure was used for global energy optimization. The BPMC global energy optimization method consists of the following steps: (1) a random conformation change of the free variables according to a predefined continuous probability distribution, (2) local energy minimization of analytical differentiable terms, (3) calculation of the complete energy including non-differentiable terms such us entropy and solvation energy, (4) acceptance or rejection of the total energy based on the Metropolis criterion and return to step 1. The binding between **1**, **2**, or 2-appt and DNA molecule was evaluated in terms of the binding energy, where the energy reflects the quality of the complex and includes grid energy, continuum electrostatic, and entropy terms. The DNA crystal structure (PDB code 423D), which contained 12 base pairs (8 G−C base pairs) and more than 800 atoms, was downloaded from Protein Data Bank. In the docking analysis, the binding site was assigned across the entire major and minor grooves of the DNA molecule. ICM docking was performed to find the most favorable orientation. The resulting **1**/**2**−DNA complex trajectories were energy minimized, and the interaction energies were computed.

Confocal Microscopy. KB-3-1 cells treated with **1**·$(PF_6)_2$ (50 μM) or cisplatin (22 μM) for 72 h were incubated in 5% CO_2 at 37 °C. The treated and untreated (as control) cells (1 mL) were stained with an acridine orange (AO)/ethidium bromide (EB) solution (40 μL, 50 mg/mL AO, 50 mg/mL EB in phosphate buffer) and then examined by laser confocal microscopy (Zeiss Axiovert 100M).

Flow Cytometric Analysis. Flow cytometry measurements were performed with an EPICS XL cytometer (Coulter Corporation, Miami, FL) equipped with an argon laser. The sheath fluid was an isotonic solution (Isoflow Coulter 8547008, Coulter Corporation). An excitation wavelength of 488 nm at 15 mW was used. About 10 000 cells were analyzed for each sample.

HeLa cells were cultured to a density of $\sim 2 \times 10^5$ cells/mL, and then **1**·$(PF_6)_2$ (50 μM) or Staurosporin Streptomyces (as a positive control) were added. Cells were incubated in 5% CO_2 at 37 °C, and were collected at 12- and 18-h intervals. The DNA was extracted according to a previously described procedure[11] and evaluated using an Annexin V protocol.

Cellular Uptake Studies. Cellular uptake experiments were conducted according to a literature method with some modifications.[22b] HeLa cells (5×10^4 cells) were seeded in 60-mm tissue culture dishes containing culture medium (2 mL/well) and incubated at 37 °C in an atmosphere of 5% CO_2/95% air for 24 h. The culture medium was removed and replaced with medium containing the ruthenium or rhenium complex at a concentration of 5, 25, or 50 μM. After exposure to the ruthenium or rhenium complex for 2 h, the medium was removed, and the cell monolayer was washed four times with ice-cold PBS. Milli-Q water (500 mL) was added, and the cell monolayer was scraped off the culture dish. Samples (300 mL) were digested in 70% HNO_3 (500 mL) at 70 °C for 2 h and then diluted 1:100 in water for inductively coupled plasma mass spectrometry (ICP−MS) analysis.

Results and Discussion

Mingos and co-workers previously reported the use of pyridyl-2,4-diamino-1,3,5-triazines as H-bonding scaffolds for the construction of metal complexes for crystal engineering studies.[13] Following the reported procedure,[13] we prepared 2-amino-4-phenylamino-6-(2-pyridyl)-1,3,5-triazine (2-appt) through the condensation of 1-phenylbiguanide with 2-pyrdinecarboxamide in alkaline methanol. The reaction of 2-appt with *cis*-$[Ru(^tBu_2bpy)_2(acetone)_2]^{2+}$ and $[Re(CO)_5Cl]$ gave **1**·$(PF_6)_2$ and **2** in yields of 70% and 84%, respectively.

The structures of **1**·$(PF_6)_2$ and **2** were established by X-ray crystallography. The metal−ligand bonding parameters for both complexes are comparable to those previously reported for ruthenium(II) and rhenium(I) diimine complexes.[23,24] In **2**, the Re(1)−N(1) and Re(1)−N(2) distances are 2.167(6) and 2.200(4) Å, respectively (Figure 2), which are close to the related Re−N distances of 2.18(1) and 2.20(1) Å in $[Re(dppz)(CO)_3(py)](O_3SCF_3)$.[25] As shown in the crystal structure of **2** (Figure 2), the Cl(1)-to-H(3) contact distance is 2.18 Å, suggesting the presence of an intermolecular hydrogen bond. The ^{1}H NMR spectra of **1**·$(PF_6)_2$ and **2** contain the expected numbers of proton signals; however, extensive overlapping of the ^{1}H signals in the aromatic region renders complete spectral assignment difficult.

The absorption spectrum of **1**·$(PF_6)_2$ in acetonitrile includes a broad absorption at 450 nm that is assigned to the $[d_\pi(Ru) \rightarrow \pi^*(diimine)]$ MLCT transition.[26] Complex **2** exhibits two absorption bands with λ_{max} (ϵ_{max}/dm^3 mol^{-1} cm^{-1}) at 376 nm (sh, 5.9×10^3) and 266 nm (3.0×10^4) in acetonitrile. Previous studies on rhenium(I)−diimine complexes have revealed that the $[Re^I \rightarrow \pi^*(diimine)]$ transition is solvent-sensitive.[27] However, changing the solvent from MeCN to MeOH or EtOH does not affect the absorption peak maximum of **2** at $\sim$376 nm (Table 2), indicating that it corresponds to an intraligand transition.

Excitation of **1**·$(PF_6)_2$ (50 μM) at 450 nm in acetonitrile resulted in a weak emission with λ_{max} at 646 nm and a

(23) Yam, V. W. W.; Lo, K. K. W.; Cheung, K. K.; Kong, R. Y. C. *J. Chem. Soc., Chem. Commun.* **1995**, 1191.
(24) Farah, A. A.; Stynes, D. V.; Pietro, W. J. *Inorg. Chim. Acta* **2003**, *343*, 295.
(25) Yam, V. W. W.; Lo, K. K. W.; Cheung, K. K.; Kong, R. Y. C. *J. Chem. Soc., Dalton Trans.* **1997**, 2067.
(26) Hartshorn, R. M.; Barton, J. K. *J. Am. Chem. Soc.* **1992**, *114*, 5919.
(27) Wrighton, M.; Morse, D. L. *J. Am. Chem. Soc*. **1974**, *96*, 998.

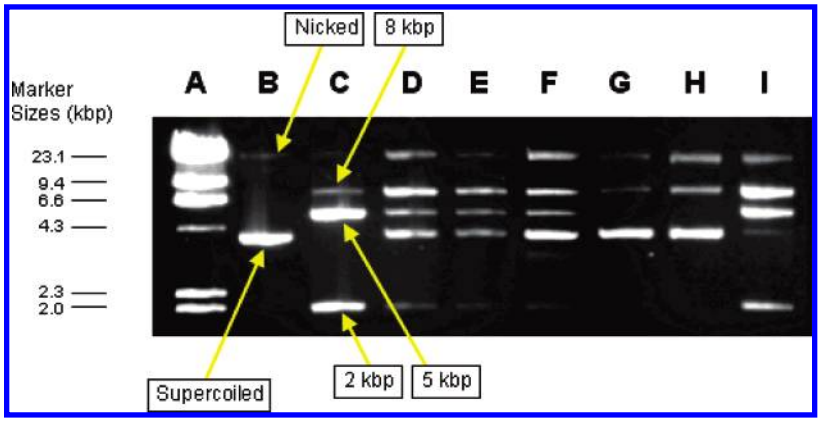

Figure 3. Inhibition of plasmid *Apa* I (restriction endonuclease) digestion of pDR2 (10.7 kbp, 21 nM bp^{-1}) by various small molecules. Lane A is size marker. Lanes B and C are undigested and *Apa* I (1 unit/μl) digested products of pDR2, respectively. Lanes D−F are the digested products of pDR2 in the presence of ethidium bromide (4 μM) (lane D), Hoechst 33342 (200 mM) (lane E), and cisplatin (200 mM) (lane F). Lanes G−I are the digested products of pDR2 in the presence of **1**·$(PF_6)_2$ at 100 mM (lane G), 20 mM (lane H), and 2 mM (lane I).

quantum yield of 0.001 with a lifetime of <0.1 μs. In ethanol, the emission λ_{max} value changes to 635 nm (see Table 2). In frozen acetonitrile solution at 77 K, λ_{max} blue shifts to 613 nm (Figure S3). With reference to previous work,[26] the 646-nm emission at 298 K was attributed to a ^{3}MLCT transition. Complex **2** is not emissive in fluid solutions at 298 K. The solid-state emissions of **1**·$(PF_6)_2$ and **2** at 298 K occur at λ_{max} 649 and 560 nm, which blue shift to 618 and 536 nm, respectively, at 77 K.

Restriction Endonuclease Fragmentation Assay. Restriction endonucleases cleave double-stranded DNA at specific sites within or adjacent to a recognition site. For example, the restriction enzyme *Apa* I recognizes the sequence

GGGCCC
CCCGGG

in double-stranded DNA and cleaves it as follows

5′-NNNNNGGGCC↓CNNNNN-3′
3′-NNNNNC↓CCGGGNNNNN-5′

Once the conformation of DNA is changed upon binding to a metal complex, the restriction enzyme cannot recognize the DNA, resulting in very little or no DNA cleavage.[20] Thus, restriction enzyme activity is strongly dependent on the local conformation of DNA at the restriction site. An agarose gel revealing the products formed after the restriction digestion (*Apa* I) of plasmid pDR2, both in the absence and in the presence of **1**·$(PF_6)_2$ or **2**, is shown in Figure 3. Two bands corresponding to the supercoiled (80.4%) and nicked (19.6%) plasmid DNA were observed for the undigested DNA (lane B). After *Apa* I digestion, three bands corresponding to DNA fragments of pDR2 with 8 kbp (13.7%), 5 kbp (44.8%), and 2 kbp (31.8%) were obtained (lane C). In the presence of ethidium bromide (intercalator, 4 μM), Hoechst 33342 (minor groove binder, 200 μM), or cisplatin (200 μM), the digestion of DNA was incomplete, and bands corresponding to the undigested plasmid DNA were also observed (see lanes D−F). The percentages of cleavage are listed in Table 3. When a higher concentration of **1**·$(PF_6)_2$ (100 μM) was used (lane G), there was complete inhibition of *Apa* I digestion (nicked + supercoiled DNA = 67.4%), whereas partial enzyme inhibition was observed at a lower concentration (20 μM) (lane H). When 2 μM of **1**·$(PF_6)_2$ was added, three bands corresponding to DNA fragments of 8 kbp (49.2%), 5 kbp (34.6%), and 2 kbp (11.8%) were obtained (lane I), suggesting that there was very little inhibition. At a concentration of 200 μM, precipitation of DNA started. Similar findings were obtained for **2** (Table 3). Given the fact that Hoechst 33342 preferentially binds to AT sequences of double-stranded DNA whereas ethidium bromide preferentially binds to GC sequences, it is not unreasonable to find that a much higher concentration of Hoechst 33342 (200 μM) than of ethidium bromide (4 μM) is required to inhibit *Apa* I. This is attributed to the restriction enzyme *Apa* I, which specifically recognizes the GC-rich sequence in double-stranded DNA. Thus, the requirement of a higher concentration (20 μM) of **1** or **2** than of ethidium bromide (GC sequence specificity) to inhibit the restriction enzyme *Apa* I can be explained by the findings described in the later section that **1** or **2** showed preference toward binding to AT sequences.

Table 3. Amount of Cleavage (%) by the Restriction Endonuclease *Apa* I in the Presence of Ethidium Bromide, Hoechst 33342, Cisplatin, **1**·$(PF_6)_2$, and **2**

	amount of cleavage (%)		
complex	8 kbp	5 kbp	2 kbp
untreated control	13.7	44.8	31.8
ethidium bromide (4 μM)	30.2	15.0	11.8
Hoechst 33342 (200 μM)	24.6	17.7	15.7
cisplatin (200 μM)	18.1	12.3	8.3
1·$(PF_6)_2$ (100 μM)	15.7	10.3	6.6
1·$(PF_6)_2$ (20 μM)	27.9	7.9	2.7
1·$(PF_6)_2$ (2 μM)	49.2	34.6	11.8
2 (100 μM)	13.6	8.4	6.4
2 (20 μM)	28.1	8.4	2.7
2 (2 μM)	48.5	35.3	11.1

Absorption Titration. As shown in Figure 4, the addition of ct DNA (0−2000 μM bp^{-1}) to **1**·$(PF_6)_2$ led to isosbestic spectral changes (isosbestic points at 297 and 555 nm) with 29% hypochromism of the 450-nm band. For the absorbance data at 450 nm, a plot of $D/\Delta\epsilon_{ap}$ vs D is shown in the inset

Table 4. Summary of DNA Binding Data for $\mathbf{1}\cdot(PF_6)_2$ and **2**

	K at 20 °C/dm^3 mol^{-1}			hypochromicity/%		
complex	ct DNA	poly(dA−dT)$_2$	poly(dG−dC)$_2$	ct DNA	poly(dA−dT)$_2$	poly(dG−dC)$_2$
$\mathbf{1}\cdot(PF_6)_2$	$(8.9 \pm 0.5) \times 10^4$	$(5.9 \pm 0.4) \times 10^5$	$(5.1 \pm 0.2) \times 10^4$	29	34	30
2	$(3.6 \pm 0.1) \times 10^4$	$(1.9 \pm 0.2) \times 10^5$	$(4.2 \pm 0.6) \times 10^4$	5	5	4

of Figure 4. This plot indicates that there is a linear relationship, with a K value of $(8.9 \pm 0.5) \times 10^4$ dm^3 mol^{-1}. The results are summarized in Table 4.

The binding of **2** to ct DNA also led to isosbestic spectral changes, with isosbestic points at 297 and 442 nm. For the 370-nm absorption band, 5% hypochromicity was observed. The K value for **2** was calculated to be $(3.6 \pm 0.1) \times 10^4$ dm^3 mol^{-1}.

Previously, Thorp and co-workers have reported a sophisticated mathematical model for the determination of binding constants (K) of greater magnitude than those obtained in this work.[28] Because of the relatively small changes in absorbance, attempts to fit the data using Thorp's model were not successful. Nevertheless, the data shown in Figure 4 fit well to eq 1, which is based on the assumption that the DNA concentration is much greater than that of the metal complex.[29]

The K values for $\mathbf{1}\cdot(PF_6)_2$ and **2** are smaller than those for ethidium bromide (intercalator) and Hoechst 33342 (groove binder), but comparable to those for other metal complexes including $[Pt(terpy)py]^{2+}$ (3.5×10^4 dm^3 mol^{-1}),[30] Δ-$[Ru(phen)_3]^{2+}$ (4.9×10^4 dm^3 mol^{-1}),[31] Λ-$[Ru(phen)_3]^{2+}$ (2.8×10^4 dm^3 mol^{-1}),[31] $[Ru(Me_2bpy)(bpy)_2]^{2+}$ (0.9×10^4 dm^3 mol^{-1}),[18d] $[Ru(phen)_2(phi)]^{2+}$ (4.7×10^4 dm^3 mol^{-1}; phen = 1,10-phenanthroline and phi = 9,10-phenanthrenequinonediimine),[32] and $[Re(dppn)(CO)_3(py)]^+$ (6.4×10^4 dm^3 mol^{-1}; dppn = benzo[*i*]dipyrido[3,2-a:2′,3′-c]phenazine).[25] Complex **1** is a dication and **2** is a neutral complex; thus, the former is expected to have a much higher binding constant, as a result of electrostatic interactions with the DNA. However, the K value for **1** is only ≤ 3 times that for **2** (Table 4). This indicates that, for $\mathbf{1}\cdot(PF_6)_2$ and **2**, other mode(s) of binding to DNA, other than electrostatic interactions, might be operative.

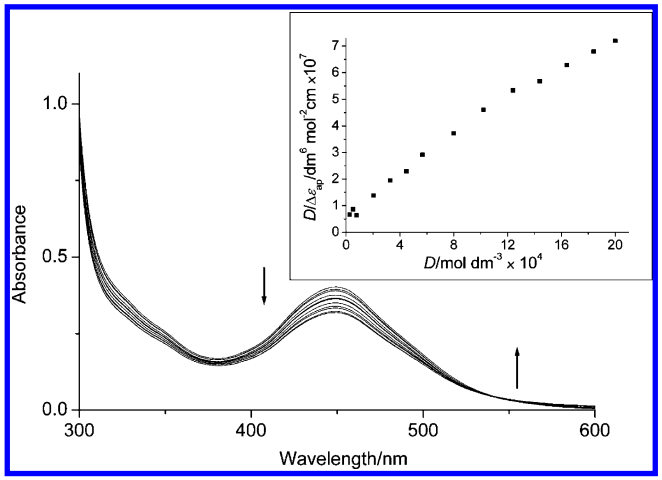

Figure 4. UV−vis spectra of $\mathbf{1}\cdot(PF_6)_2$ (50 μM) in Tris buffer with [DNA]/[$\mathbf{1}\cdot(PF_6)_2$] ratios of 0−40 at 20 °C. Inset: Plot of $D/\Delta\epsilon_{ap}$ vs D. Absorbance was monitored at 450 nm.

A shift in absorption maximum and large hypochromic effects have often been cited as indicators for intercalative binding. In this work, the binding of $\mathbf{1}\cdot(PF_6)_2$ or **2** to DNA led to modest hypochromicity, but there were negligible shifts in the absorption maxima. Furthermore, the low binding constants of $\sim 10^4$ suggest that the interactions between these two metal complexes and DNA might not be intercalative in nature.

Complex **2** is nonemissive in Tris buffer or acetonitrile. Although $\mathbf{1}\cdot(PF_6)_2$ is emissive in degassed acetonitrile solution, binding of $\mathbf{1}\cdot(PF_6)_2$ to ct DNA did not lead to any change in its emission intensities. Thus, emission spectroscopy could not be used to examine the binding properties of $\mathbf{1}\cdot(PF_6)_2$ or **2**.

Viscosity Experiments. Viscosity measurements are ionic-strength- and concentration-dependent; consequently, we used buffers of the same ionic strength for all measurements.[18] Because of the low solubility of $\mathbf{1}\cdot(PF_6)_2$ and **2** in aqueous buffers, [complex]/[DNA] ratios of ≤ 0.12 were used in the viscosity experiments. The plots of $(\eta/\eta_o)^{1/3}$ vs binding ratio (r-bound) for $\mathbf{1}\cdot(PF_6)_2$, **2**, ethidium bromide (an intercalator), and Hoechst 33342 (a groove binder) are shown in Figure 5. The ct DNA viscosity did not increase when the concentration of $\mathbf{1}\cdot(PF_6)_2$ or **2** was raised. However, when the concentration of ethidium bromide was increased, a substantial increase in ct DNA viscosity was observed. This can be rationalized by a lengthening of the DNA duplex upon the insertion of ethidium bromide molecules between the stacked bases. The insignificant changes in DNA viscosity for $\mathbf{1}\cdot(PF_6)_2$ and **2** provide additional evidence indicating that their mode of binding to DNA is not intercalative in nature.

(28) (a) Carter, M. T.; Rodriguez, M.; Bard, A. J. *J. Am. Chem. Soc.* **1989**, *111*, 8901. (b) Kalsbeck, W. A.; Thorp, H. H. *J. Am. Chem. Soc.* **1993**, *115*, 7146. (c) Smith, S. R.; Neyhart, G. A.; Kalsbeck, W. A.; Thorp, H. H. *New J. Chem.* **1994**, *18*, 397.
(29) Li, H. J.; Crothers, D. M. *J. Mol. Biol.* **1969**, *39*, 461.
(30) Cusumano, M.; Di Pietro, M. L.; Giannetto, A. *Inorg. Chem.* **1999**, *38*, 1754.
(31) (a) Yamagishi, A. *J. Chem. Soc., Chem. Commun.* **1983**, 572. (b) Barton, J. K.; Danishefsky, A. T.; Goldberg, J. M. *J. Am. Chem. Soc.* **1984**, *106*, 2172. (c) Barton, J. K.; Goldberg, J. M.; Kumar, C. V.; Turro, N. J. *J. Am. Chem. Soc.* **1986**, *108*, 2081. (d) Gorner, H.; Tossi, A. B.; Stradowski, C.; Schulte-Frohlinde, D. *J. Photochem. Photobiol. B* **1988**, *2*, 67. (e) Hiort, C.; Norden, B.; Rodger, A. *J. Am. Chem. Soc.* **1990**, *112*, 1971. (f) Haworth, I. S.; Elcock, A. H.; Freeman, J.; Rodger, A.; Richards, W. G. *J. Biomol. Struct. Dyn.* **1991**, *9*, 23. (g) Satyanarayana, S.; Dabrowiak, J. C.; Chaires, J. B. *Biochemistry* **1992**, *31*, 9319. (h) Satyanarayana, S.; Dabrowiak, J. C.; Chaires, J. B. *Biochemistry* **1993**, *32*, 2573. (i) Eriksson, M.; Leijon, M.; Hiort, C.; Norden, B.; Graslund, A. *Biochemistry* **1994**, *33*, 5031. (j) Choi, S. D.; Kim, M. S.; Kim, S. K.; Lincoln, P.; Tuite, E.; Norden, B. *Biochemistry* **1997**, *36*, 214. (k) Collins, J. G.; Sleeman, A. D.; Aldrich-Wright, J. R.; Greguric, I.; Hambley, T. W. *Inorg. Chem.* **1998**, *37*, 3133. (l) Coggan, D. Z. M.; Haworth, I. S.; Bates, P. J.; Robinson, A.; Rodger, A. *Inorg. Chem.* **1999**, *38*, 4486.
(32) Pyle, A. M.; Rehmann, J. P.; Meshoyrer, R.; Kumar, C. V.; Turro, N. J.; Barton, J. K. *J. Am. Chem. Soc.* **1989**, *111*, 3051.

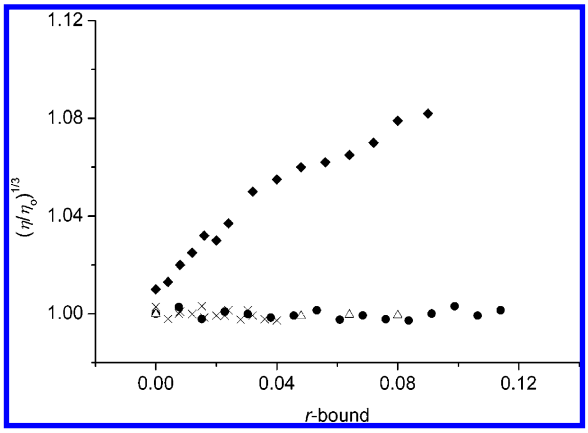

Figure 5. Relative specific viscosities of calf thymus DNA in the presence of ethidium bromide (♦), Hoechst 33342 (●), **1**·$(PF_6)_2$ (×), and **2** (△), shown as a function of the binding ratio (*r*-bound).

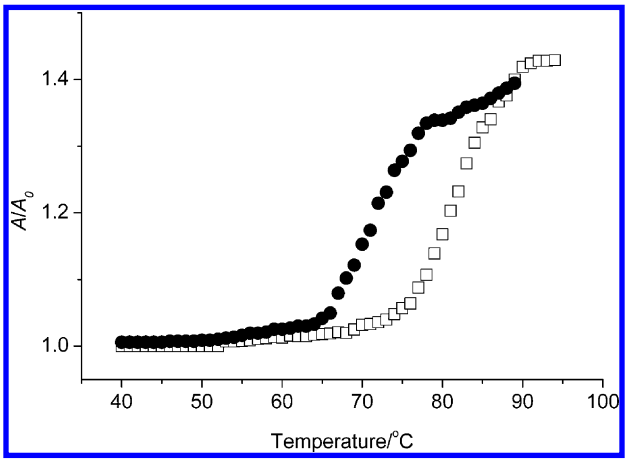

Figure 6. Plots of A/A_0 vs temperature for 33-bp DNA (20 μM) (●) and 33-bp DNA in the presence of **1**·$(PF_6)_2$ (□) with a 1:1 ratio of DNA base pairs to **1**·$(PF_6)_2$, both in Tris buffer.

We did not use DNA unwinding experiments to further study the binding mode, as Dougherty and Pilbrow have previously shown that the promotion of DNA unwinding is not a definitive indication for intercalation.[33] The best example of such a case is the dicationic steroid irehdiamine A, which is not an intercalative DNA binding agent but was found to unwind DNA.[34]

DNA Melting Study. The DNA melting curves for a 33-bp double-helical DNA molecule (50 μM bp^{-1}) in the absence and presence of **1**·$(PF_6)_2$ (50 μM) are shown in Figure 6. Compared to the untreated DNA (T_m = 71 °C), the melting temperature increased to ca. 83 °C upon treatment with either **1**·$(PF_6)_2$ or **2**. After the temperature had been increased to 90 °C, spectral hyperchromism was observed for **1**·$(PF_6)_2$ (213 and 260 nm) and **2** (215 and 259 nm), with isosbestic points at 305 and 365 nm for **1**·$(PF_6)_2$ and 300 nm for **2**. Because the increases in DNA melting temperature (ΔT_m = +12 °C) are similar in both cases, we infer that the increase in the stability of the helical DNA structure after the binding of **1**·$(PF_6)_2$ is similar to that for **2**.

Binding to Synthetic Oligonucleotides. We observed no enhancement in emission intensity upon the addition of poly-(dA−dT)$_2$ or poly(dG−dC)$_2$ to a Tris buffer solution of **1**·$(PF_6)_2$ or **2**. The binding of **1**·$(PF_6)_2$ to poly(dA−dT)$_2$ and poly(dG−dC)$_2$ resulted in similar UV−vis spectral changes (Figure S4). Hypochromicity was found to be 5−34%, and the binding constants for **1**·$(PF_6)_2$ and **2** with poly(dA−dT)$_2$ were determined to be (5.9 ± 0.4) × 10^5 and (1.9 ± 0.2) × 10^5 dm^3 mol^{-1}, respectively. These values are about an order of magnitude larger than those for poly(dG−dC)$_2$ [(5.1 ± 0.2) × 10^4 dm^3 mol^{-1} for **1**·$(PF_6)_2$, (4.2 ± 0.6) × 10^4 dm^3 mol^{-1} for **2**; Table 4). Thus, **1**·$(PF_6)_2$ and **2** preferentially bind to AT sequences.

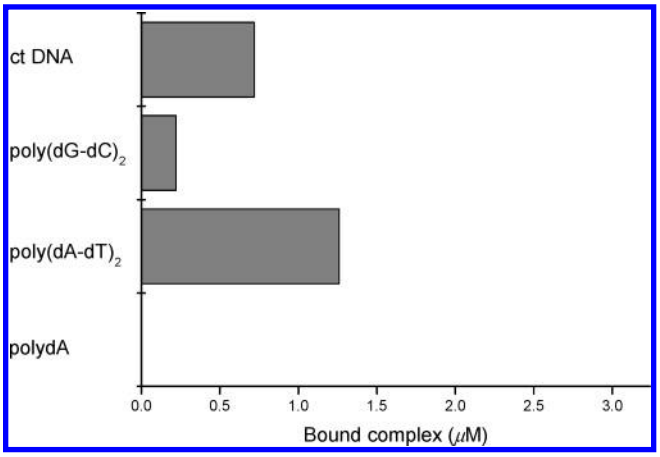

Figure 7. Competition dialysis results: Concentrations of bound **1**·$(PF_6)_2$ bound to various nucleic acid molecules.

UV melting experiments with poly(dA−dT)$_2$ and poly-(dG−dC)$_2$ also revealed a general preference for binding to AT sequences. In the presence of **1**·$(PF_6)_2$ or **2**, the melting temperature of poly(dA−dT)$_2$ increased from 56.6 to 77.0 °C. In contrast, we found that, for poly(dG−dC)$_2$, the melting temperature increased by less than 1 °C (the melting temperature changed from 73.9 to 74.8 °C for **1**·$(PF_6)_2$ and to 74.3 °C for **2**) under similar experimental conditions.

Competition Dialysis. Complex **1**·$(PF_6)_2$ showed a strong preference for binding to poly(dA−dT)$_2$, whereas no binding to single-stranded DNA (polydA) was observed (Figure 7). Similar findings were observed for **2**.

The binding constants *K* for the interaction between **1**·$(PF_6)_2$ or **2** and poly(dA−dT)$_2$ are larger than those obtained with poly(dG−dC)$_2$, revealing a specificity for AT base pair binding. This can be attributed to H-bonding and van der Waals interactions between the metal complexes and the AT-rich regions of DNA. The NH and NH_2 groups in **1**·$(PF_6)_2$ and **2** can play an important role in the interaction between these two metal complexes and the minor groove of DNA regions that are AT-rich. For minor groove binders such as Hoechst 33258,[35] more favorable electrostatic interactions are observed for AT-rich regions, which have

(33) Dougherty, G.; Pilbrow, J. R. *Int. J. Biochem.* **1984**, *16*, 1179.

(34) Waring, M. J.; Henley, S. M. *Nucleic Acids Res.* **1975**, *2*, 567.

(35) (a) Kelly, J. M.; McConnell, D. J.; OhUigin, C.; Tossi, A. B.; Kirsch-De Mesmaeker, A.; Masschelein, A.; Nasielski, J. *J. Chem. Soc., Chem. Commum.* **1987**, 1821. (b) Kirsch-De, Mesmaeker, A.; Orellana, G.; Barton, J. K.; Turro, N. J. *Photochem. Photobiol.* **1990**, *52*, 461. (c) Orellana, G.; Kirsch-De, Mesmaeker, A.; Barton, J. K.; Turro, N. J. *Photochem. Photobiol.* **1991**, *54*, 499. (d) Feeney, M. M.; Kelly, J. M.; Tossi, A. B.; Kirsch-De, Mesmaeker, A.; Lecomte, J. P. *J. Photochem. Photobiol. B* **1994**, *23*, 69.

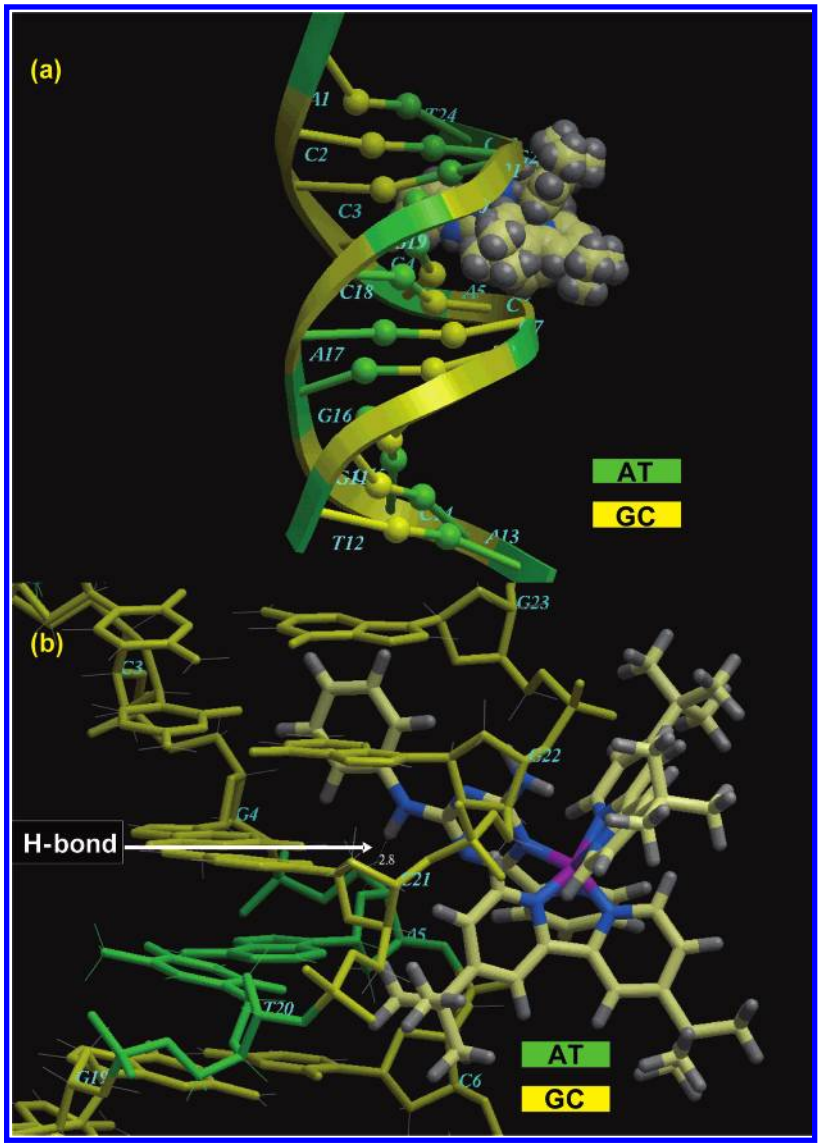

Figure 8. (a) Molecular modeling of **1**·$(PF_6)_2$ with B-DNA (PDB code 423D). (b) H-bonding interaction between **1** and B-DNA.

Table 5. Cytotoxicities of **1**·$(PF_6)_2$ and **2** toward Human Cancer Cell Lines, as well as Noncancerous Normal Lung Fibroblasts (CCD-19Lu)

	$IC_{50}/\mu M$				
complex	KB-3-1	KB-V-1	HepG2	HeLa	CCD-19Lu
control(4% DMSO)	>200	>200	>200	>200	>200
1·$(PF_6)_2$	52.3 ± 3.4	199 ± 3	30.2 ± 6	59.7 ± 0.5	151 ± 3
2	43.5 ± 2.2	195 ± 1	30.9 ± 1.1	50.3 ± 0.2	112 ± 3
cisplatin	22.1 ± 3.6	39.1 ± 1.7	10.5 ± 0.5	11.6 ± 0.2	129 ± 1

greater negative electrostatic potentials than DNA stretches that are rich in GC.

Molecular Modeling. The results of spectroscopic titrations and viscosity experiments suggest that **1**·$(PF_6)_2$ or **2** does not interact with DNA via intercalation. To provide further insight into the possible modes of interaction, we examined the binding of **1**·$(PF_6)_2$, **2**, and 2-appt toward DNA using molecular modeling (ICM).[36] Complex **1** exhibits the highest binding interaction (as revealed by the calculated binding energy of −57.84 kcal mol^{-1}) toward B-DNA, and as shown in Figure 8a, it is located close to the AT-rich sequence of the minor groove. This finding is consistent with the proposed specificity from the spectroscopic titrations and competitive dialysis experiments. The optimal binding conformations in the minor groove through H-bonding interactions are shown in Figure 8b. It can be seen in this figure that **1** fits the groove shape well, forming an extensive hydrogen-bonding network. Similar modes of binding were observed for the interactions of **2** and 2-appt with B-DNA, with both binding to AT-rich stretches in the minor groove and with **2** having a relatively lower calculated binding energy (−46.58 vs −56.52 kcal mol^{-1}; Figures S5 and S6). The results indicate that the effects, due either to the

(36) Totrov, M.; Abagyan, R. *Proteins, Suppl.* **1997**, *1*, 215.

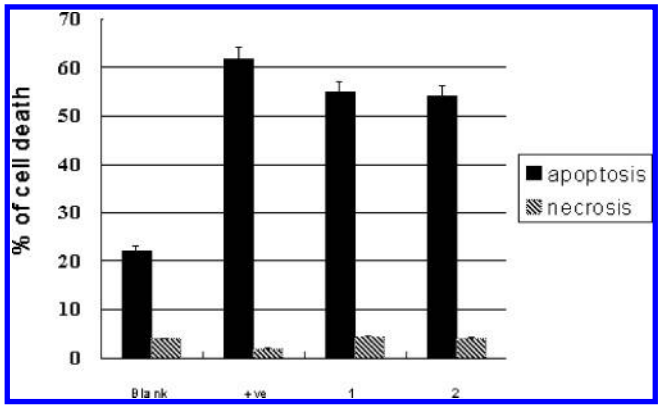

Figure 9. Percentages of cell death for HeLa cells induced by **1**·$(PF_6)_2$ and **2** after 12 h of incubation. Staurosporin Streptomyces was used as a positive control.

ruthenium/rhenium atoms or the ancillary ligands other than 2-appt, do not significantly impede the formation of H-bonds between the complexes and DNA.

Cytotoxicity Tests (MTT Assay). The cytotoxicities of **1**·$(PF_6)_2$ and **2** against four human carcinoma cell lines (KB-3-1, KB-V-1, HepG2, HeLa) and a noncancerous CCD-19Lu cell line were studied, with the results listed in Table 5. Using the MTT assay, the IC_{50} values were calculated from the numbers of cells that survived at each particular complex concentration, after exposure for 48 h. The IC_{50} values (final concentration ≤4% DMSO) were found to be in the following order: cisplatin < **1**·$(PF_6)_2$ ≈ **2**. There were no significant variations in the IC_{50} values for either **1**·$(PF_6)_2$ or **2** between the various cell lines. The complexes exhibited significant potency against the multi-drug-resistant KB-V-1 cell line, but were less toxic toward the noncancerous CCD-19Lu cell line. Because of the production of lactic acid, a slightly acidic milieu of pH 6.8 is frequently encountered in solid tumors, as compared to a pH of 7.2−7.4 in normal tissues. For comparative purposes, we performed cytotoxicity tests with **1**·$(PF_6)_2$ and **2** in a HeLa cell line at pH 6.8. Results indicated that there were no significant variations in the IC_{50} values (∼50 μM) obtained at pH 6.8, compared to those determined at pH 7.2−7.4 (∼50−60 μM).

Confocal Microscopy and Flow Cytometric Analysis. The cell death induced by **1**·$(PF_6)_2$ and **2** was quantitatively examined by flow cytometry using the Annexin V protocol.[11] On the basis of their overall cell morphology and cell membrane integrity, necrotic and apoptotic cells could be distinguished from one another using laser confocal microscopy.[20,37] In the absence of cisplatin or **1**·$(PF_6)_2$ (Figure S7), the nuclei of living cells were stained bright green in spots. However, after treatment with either cisplatin or **1**·$(PF_6)_2$, green apoptotic cells containing apoptotic bodies, as well as red necrotic cells, were observed. As shown in Figure 9, **1**·$(PF_6)_2$ and **2** were found to induce 50−60% apoptosis, with less than 5% necrosis detected. The results show that **1**·$(PF_6)_2$, like cisplatin, can induce apoptosis in the KB-3-1 cell line. Analogous results were observed for **2**.

Cellular Uptake Studies. Cellular uptake studies were performed to ascertain whether the cytotoxicity results correlated with cellular levels. The accumulation of **1** and **2** in HeLa cells is shown in Figure S8. The results suggested that **1** and **2** were accumulated in HeLa cells to approximately equal extents. Both **1** and **2** could effectively enter the cancer cell, and the cellular uptake levels were dependent on the dose of each complex used. This also indicates that their cytotoxicities as determined by MTT assays were not disproportionately influenced by the complexes having different cellular uptake levels.

Conclusions

[Ru(^{t}Bu$_2$bpy)$_2$(2-appt)]$(PF_6)_2$ [**1**·$(PF_6)_2$, ^{t}Bu$_2$bpy = 4,4′-di-*tert*-butyl-2,2′-bipyridine, 2-appt = 2-amino-4-phenylamino-6-(2-pyridyl)-1,3,5-triazine] and [$Re(CO)_3$(2-appt)Cl] (**2**) bind to ct DNA with binding constants of $(8.9 \pm 0.5) \times 10^4$ and $(3.6 \pm 0.1) \times 10^4$ dm^3 mol^{-1}, respectively, at 20 °C. The data from UV−vis absorption titration, melting studies, and competition dialysis experiments all support a specific binding mode for **1**·$(PF_6)_2$ and **2** at AT-rich regions of DNA. The binding of **1**·$(PF_6)_2$ or **2** to DNA led to modest hypochromicity and insignificant shifts in the absorption maxima. Results from spectroscopic titrations and viscosity experiments were consistent with the complexes having low binding constants (∼10^4) and indicated that these metal complexes interact with DNA via groove binding. Modeling studies suggest that the minor groove is the favored binding site for **1** and **2**.

Complexes **1**·$(PF_6)_2$ and **2** exhibited moderate cytotoxicities toward several established human cancer cell lines, including KB-3-1, HepG2, and HeLa, and had significant activity against the multi-drug-resistant KB-V-1 cancer cell line. According to results from confocal microscopic and flow cytometric studies, **1**·$(PF_6)_2$ and **2** selectively induced apoptosis (50−60%) leading to cancer cell death, with necrosis levels generally below 5%. As the electronic structure and properties of metal complexes can be modulated through the metal ion and auxiliary ligands, we envision that metal complexes containing analogous H-bonding motifs have significant potential in the development of specific metal-based groove binders.

Acknowledgment. This work was supported by the Areas of Excellence Scheme established under the University Grants Committee of the Hong Kong Special Administrative Region, China (AoE/P-10/01); The University of Hong Kong (University Development Fund); and the Research Grants Council of Hong Kong SAR, China (CityU 1189/01P).

Supporting Information Available: Figures S1−S8 and CIF files for the crystal structures of [Ru(^{t}Bu$_2$bpy)$_2$(2-appt)]$(PF_6)_2$ [**1**·$(PF_6)_2$] and [$Re(CO)_3$(2-appt)Cl] (**2**). This material is available free of charge via the Internet at http://pubs.acs.org.

IC061518S

(37) (a) Schwartzman, R. A.; Cidlowski, J. A. *Endocr. Rev.* **1993**, *14*, 133. (b) Vermes, I.; Haanen, C. *Adv. Clin. Chem.* **1994**, *31*, 177.